

Sedimentary facies at southern marginal part: an indicator of deposition environmental fluctuation in Kathmandu basin, Nepal

Ananta P. Gajurel

Department of Geology, Tri-Chandra Campus, Tribhuvan University, Kathmandu, Nepal
(Email: apgajurel@gmail.com)

ABSTRACT

Kathmandu basin is an intermontane basin located in Kathmandu Nappe. This study focus on the basin-fill sediments deposited at the southern part of the Kathmandu basin. Lithofacies characteristics from field as well as available laboratory data were used to understand deposition environmental system in the basin. Lithofacies of sedimentary deposit in Buranchuli area exclusively represents proximal alluvial fan system having debris and normal river water current flow sediments. In contrast, lithofacies in the Pyangaon area reveals two distinct sediments: the lower fine-grained deltaic and the upper coarse-grained alluvial fan sediments. This study constrains occurrence of centennial scale lake level fluctuation evidenced from process of sedimentation. Alluvial fan is one of the major key mechanisms for the control of lake level changes in Kathmandu basin. Thus, depositional terraces of fluvio-deltaic origin at the northern part of the basin were developed as a result of modification in the alluvial fan system at the southern part of basin.

Keywords: Lake level fluctuation, lithofacies, alluvial fan, Kathmandu basin

Received: 15 November 2010

revision accepted: 7 July 2011

INTRODUCTION

Kathmandu basin is situated at the northern margin of Kathmandu Nappe (Hagen 1969) and it is a piggy-back intermontane basin transported along the Mahabharat Thrust (Stöcklin and Bhattacharya 1981) (Fig. 1). Morphologically, the basin is closer to a circular shape, which is characterized by centripetal drainage pattern (Holmes 1978). Basement rocks and surrounding mountains of the basin is consisting of Paleozoic meta-sedimentary sequence in east, west and south, and Precambrian augen gneiss and pegmatite in the north (Rai, 2001). Thus, the basin has accommodated predominant siliciclastic sediments derived from meta-sedimentary (phyllite, siltstone, shale, metasandstone and limestone) and crystalline (schist, gneiss and pegmatite) rocks and has archived up to 600 m thick sedimentary record since 3 Ma covering for about 400 km² surface area (Moribayashi and Maruo 1980; Yoshida and Gautam 1988; Bajracharya 1996; Sakai 2001). These siliciclastic sediments were accumulated as alluvial fans, fluvial and deltaic terraces at the margin to outer central part and lacustrine deposit at the central part of the basin (Yonechi 1973; Natori et al. 1980; Gajurel 1998; Sakai 2001; Sakai et al. 2006). These sediments are separated into coarse deltaic and shallow lacustrine facies, fine deltaic and deep lacustrine facies, and alluvial fan facies (Fig. 2). Stratigraphically, the basin sediments have been classified into various ways (Dhondial 1966; Yoshida and Igarashi 1984; Dongol and Brookfield 1994; Sakai 2001; Shrestha et al. 1998; Sakai et al. 2008). At southern part of the basin the sediments are classified as Boregaon, Chapagaon and

Pyangaon terrace deposits and Lukundol Formation (Yoshida and Igarashi 1984); recently the classification is being further refined by Sakai (2001) separating into Itaiti, Lukundol and Tarebhir Formations at the south, and Patan, Kalimati and Bagmati Formations at the central part of the basin. Likewise, at the northern part of Kathmandu basin, the stratigraphy is revised with details by Sakai et al. (2008). They separated the sediments into Patan, Tokha, Thimi, Gokarna, Kalimati and Dharmasthali Formations. Here the stratigraphy of the basin-fill sediments have been separated into northern, central and southern parts as earlier researchers and summarized in Table 1 and geochronological data obtained from the basin-fill sediments are compiled in Table 2. These age data set have bracketed the basin sediments into Patan (14-10 ka), Tokha (20-14 ka), Thimi (34-20 ka), and Gokarna (50-34 ka) Formations using ¹⁴C radiometric dating method. Sunakothi formation consisting of fine deltaic sediments is equivalent to Gokarna and Themi formations at south (Paudel and Sakai 2010). For the older sediments, paleomagnetic dating technique set the age boundaries for Itaiti (<730 ka), Kalimati (1 Ma-12 ka), Dharmasthali (>780 ka), Lukundol (2.5 Ma- 730 ka) and Bagmati (3-2.5 Ma) Formations. Depositional geomorphological form of the sedimentary piles have preserved as terraces, which are named as Boregaon (1,410-1,430 m), Chapagaon (1,440-1,460 m) and Pyangaon (1,480-1,520 m) at south and Patan (1,300-1,320 m), Thimi (1,330-1,340 m), and Gokarna (1,350-1,390 m) at central and northern part of the basin (Yoshida and Igarashi 1984; Sakai et al. 2008). Unfortunately, the present days' chaotic and rapid urbanization within the Kathmandu valley has

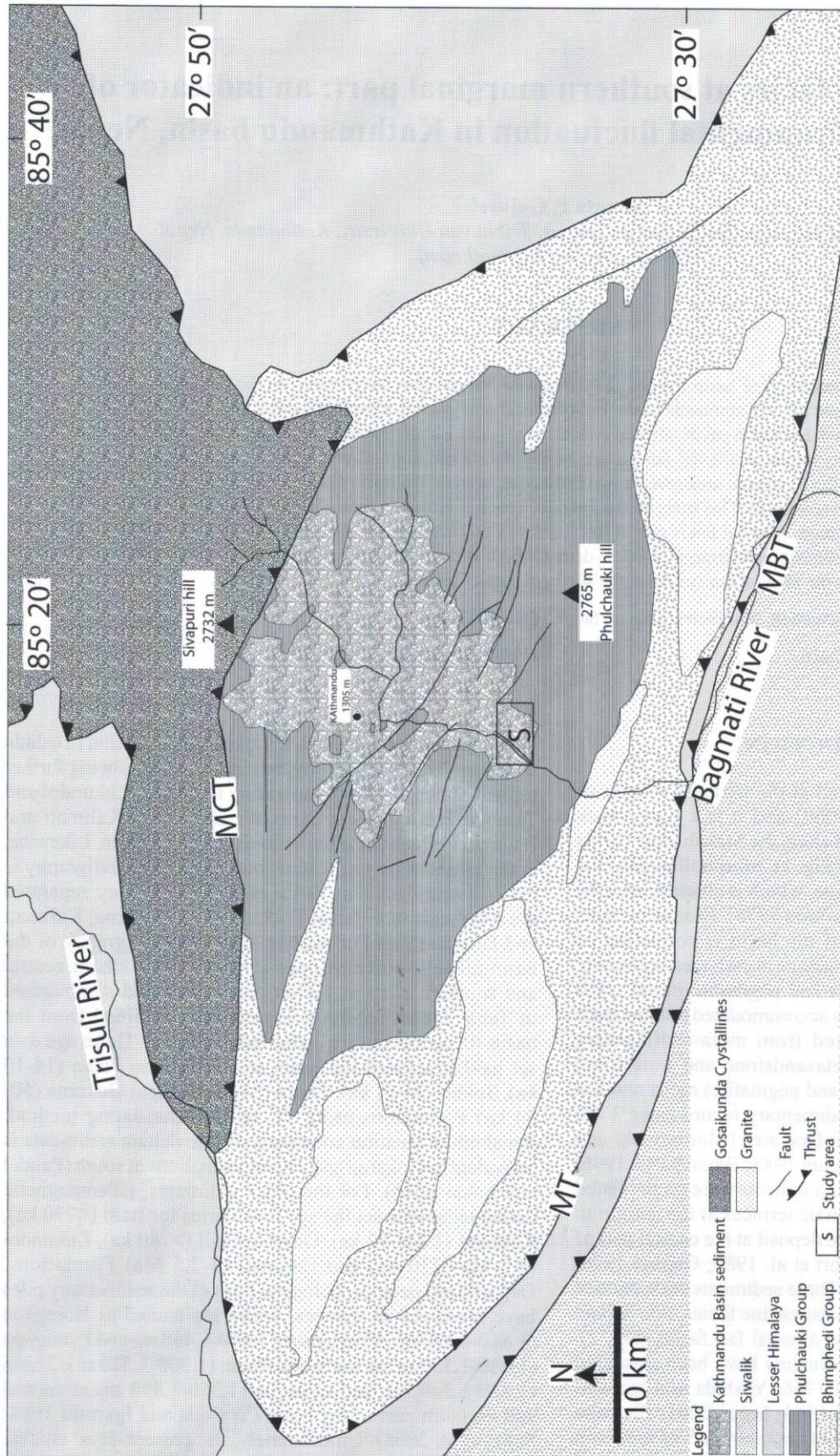


Fig. 1: Location of Kathmandu basin and the study area in the Kathmandu Nappe (modified after Rai 2001)

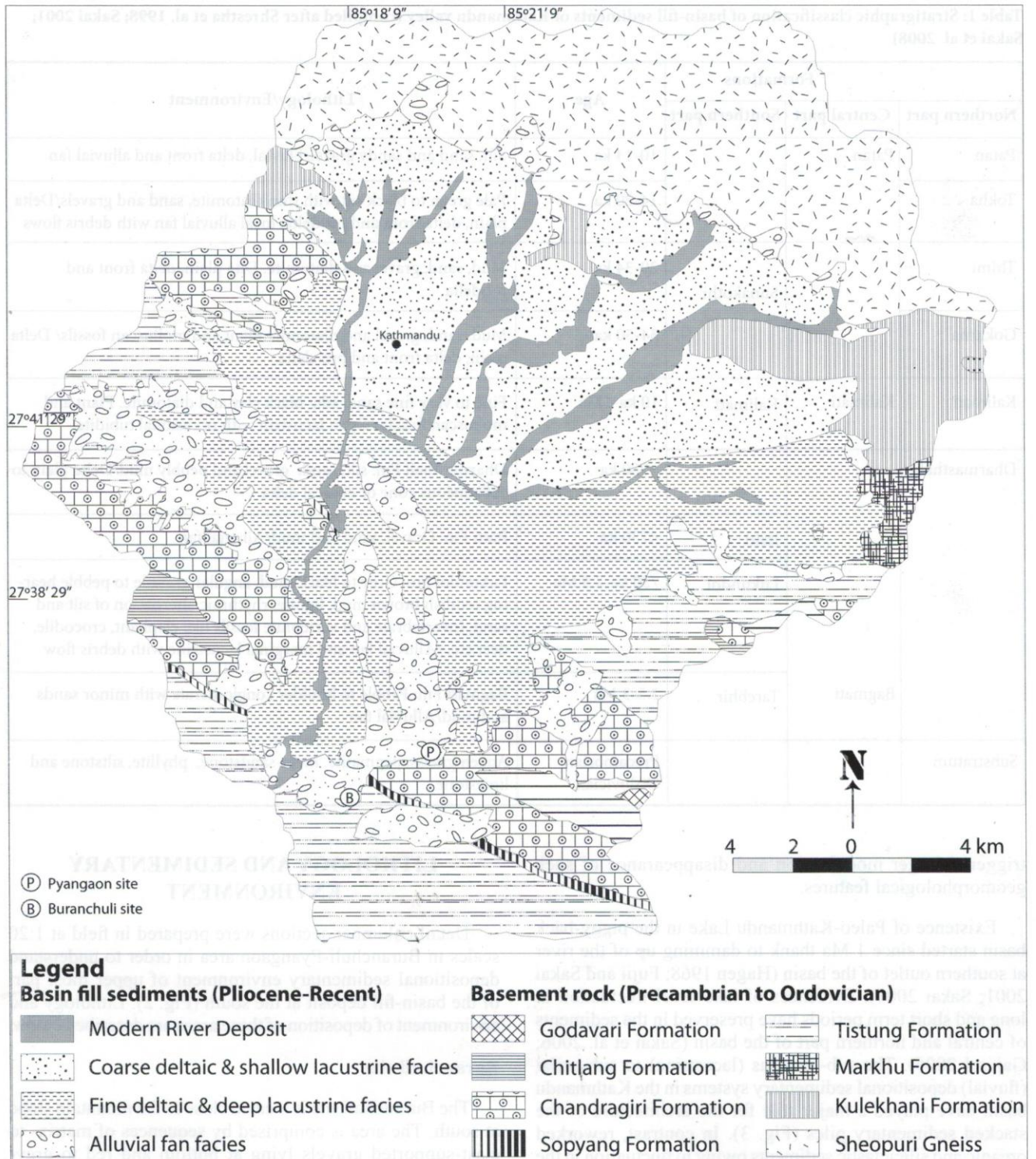


Fig. 2: Geological facies map of Kathmandu basin with geology of surrounding area (modified after Stöcklin and Bhattarai 1981; Shrestha et al. 1998; Sakai 2001; Saijo and Kimura 2007)

Table 1: Stratigraphic classification of basin-fill sediments of Kathmandu valley (compiled after Shrestha et al. 1998; Sakai 2001; Sakai et al. 2008)

Formations			Age	Lithology/Environment
Northern part	Central part	Southern part		
Patan	Patan		10-14 ka	Silt, sand and sandy gravel/Fluvial, delta front and alluvial fan
Tokha			14-20 ka	Pale green to black silt with thin diatomite, sand and gravels/Delta plain, delta front and prodelta; local alluvial fan with debris flows
Thimi		Sunakothi	20-34 ka	Mud, sand, gravel and diatomite. Delta plain, delta front and prodelta
Gokarna			34-50 ka	Mud, sand, gravel and diatomite. Plant and molluscan fossils/ Delta plain, delta front and pro-delta
Kalimati	Kalimati	Kalimati	10 ka-1Ma	Fine to very fine sand, silt, black clay and diatomite. Plant and molluscan fossils /Open lacustrine with occasional tubidite
Dharmasthali			>780 ka	Dharmasthali Fm: silt, sand, gravel and pebbly mud/Delta plain to subaqueous cone or conical delta
		Itaiti	<730 ka	Itaiti Fm: Gravel, sand and mud/Alluvial fan
		Lkundol	730 ka-2.5 Ma	Lkundol Fm: Grey to black mud, angular granule to pebble bearing reddish brown mud, lignite, rhythmic alternation of silt and sand. Invertebrate and vertebrate fossils like elephant, crocodile, deer, etc. /Alluvial fan and marginal lacustrine with debris flow
		Bagmati	Tarebhir	2.5-3 Ma
Substratum			Precambrian-Ordovician	Augen gneiss, pegmatite, meta-sandstone, phyllite, siltstone and limestone

triggered larger modification and disappearance of such geomorphological features.

Existence of Paleo-Kathmandu Lake in the piggy-back basin started since 1 Ma thanks to damming up of the river at southern outlet of the basin (Hagen 1968; Fujii and Sakai 2001; Sakai 2001). Evidences of lake level fluctuation in long and short term periods have preserved in the sediments of central and northern part of the basin (Sakai et al. 2006; Gajurel 2006). The sub-aqueous (lacustrine) to sub-aerial (fluvial) depositional sedimentary systems in the Kathmandu basin have played a major role for the architecture of the stacked sedimentary piles (Fig. 3). In contrast, reworked organic and siliciclastic sediments owing to fluctuation in the two systems as well as iso-time lines at these depositional environments complicate the geology of the basin-fill deposit. This study explores sedimentary environmental signature in the sediments at the southern part of the basin in order to understand the major deposition environmental fluctuations in the Kathmandu basin.

LITHOLOGY AND SEDIMENTARY ENVIRONMENT

Detail columnar sections were prepared in field at 1:20 scales in Buranchuli-Pyangaon area in order to understand depositional sedimentary environment of upper most part of the basin-fill deposit at the south (Fig. 2). Lithology and environment of deposition of these areas are described below.

Buranchuli site

The Buranchuli site is located close to the mountain slope at south. The area is comprised by sequences of matrix- to clast-supported gravels lying at bottom and red to grey-black mud at top (Fig. 4 and 5). Gravels are comprised by fine-grained sandstone, siltstone and limestone derived from surrounding mountain rocks. Sandy and silty layers are very rare and appear as lenses. The sequences range in thickness from 2 to 10 m and contact between sequences is sharp to slightly erosive in the mountain front area, while to the basin ward direction occasional deep erosional surfaces up to 4 m relief are formed on mud layers. Other characteristic feature

to be observed in the basin ward direction is the occasional interpenetration structure between gravel and mud layers that form lateral wedge shaped contact for more than 3 m. Depositional surfaces are inclined to 5-21° due N0-120°.

Depositional facies are separated into coarse-grained and fine-grained facies. Coarse-grained facies is predominant over the fine-grained facies.

Coarse-grained facies

Coarse-grained facies are characterized by multiple phase of unsorted to moderately sorted gravel having normal to reverse grading structures. Lensoid to tabular silty mud units separate the multiple events. Matrix is comprised by silt and clay. The coarse-grained facies are further sub-divided into matrix-supported gravel and clast-supported gravel (Fig. 5).

Matrix-supported gravel

Muddy matrix in this lithofacies has two sets of color: red to reddish brown and grey to dark grey. Matrix-supported gravel horizons are 40 to 200 cm thick and the proportion of matrix increases toward top. The horizons are normal to inversely graded and are in gradational contact with underlying clast-supported gravel and overlying red to reddish brown mud or grey to dark grey mud. The upper contact of the horizons in some case is convex upward. Occasional horizons of clast-supported lensoid gravels are accumulated within the facies without having sharp contact. The gravels are angular to sub-rounded in the proximity of mountain slope and sub-rounded to round toward basin direction and size decreases to pebble to small boulders. In some cases the matrix-supported facies is also lying within dark grey mud as lens (Fig. 5). The lithofacies is similar to top part of recent debris flow deposit observed at right bank of the Buranchuli Khola consisting of grey mud-supported gravel passes to grey mud at top that having dispersed angular to sub-rounded pebble clast (Fig. 5).

Clast-supported gravel

Clast-supported gravel horizons are mainly comprised by pebble, cobble and boulders. Average size of the gravels is represented by 60-70 cm diameter, however, occasional boulders up to 3 m are also present. Small pebbles and large cobbles to boulders are sub-angular, while large pebbles and small cobbles are rounded. Sub-rounded clasts are normally discoidal in shape. These gravels form usually unsorted and disorganized fabric. The highly unsorted gravels contain elevated and vertical boulders, which are situated close to fine-grained facies (Fig 5). Sandy granule lenses are sandwiched in this lithofacies. Massive boulder to cobble beds have reddish brown colored sand-silt-clay matrix. Gravels having moderate sorting produced weak imbrication structure.

Fine-grained facies

Fine-grain facies are appeared at top of gravel sequence and represented by sand, silt and mud. Sands are very rare, while muds are predominant. The muds are red to reddish brown and grey to black with carbonaceous matter and contain angular to sub-rounded sand, granule to pebbly clasts (Fig. 5). These facies are normally 15 to 40 cm thick. The sediment of the facies is named as diamictite by Sakai (2001).

Interpretation

The gravel horizon characterized by ungraded and disorganized fabric, vertical and elevated clasts, inverse grading i.e. pebble lying on erosion surface of mud horizon change to cobble toward top and again to up section the size decreases, and the contact at basal part having sharp to some erosional relief with underlying muddy unit is interpreted as debris flow deposit (Nemec and steel 1984; Miall 1996; Blair 1999). The debris flow sequence ranges in thickness from 2 to 10 m.

Gravels having better roundness and imbrication structures in the sequence are interpreted as high-energy stream current flow deposit. These sequences range in

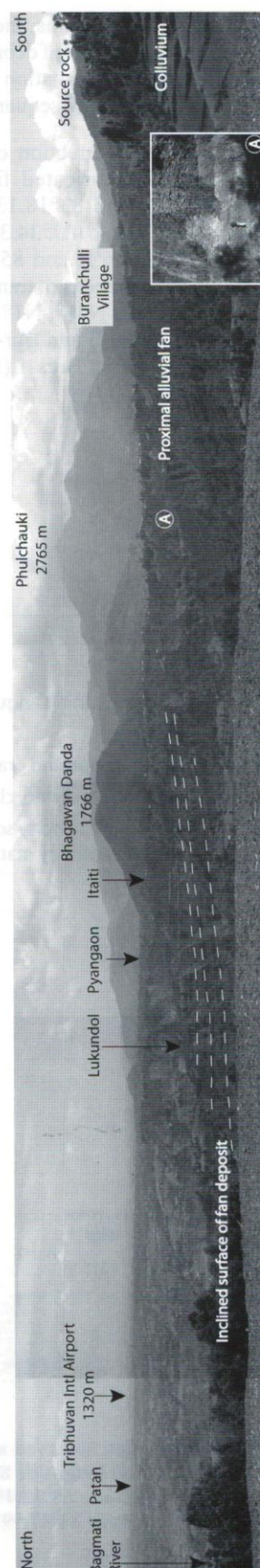


Fig. 3: Panoramic view of architecture formed by sedimentary piles in Kathmandu valley from southern part of valley towards NNE-E, inset photo marked as A is an example of exposure.

thickness from 2 to 5 m. Thus, the facies in the Buranchuli area represent an alternation of debris flow and stream current flow as well as an amalgamation of the two types of flow producing up to 10 m thick sequence.

For transportation direction of the sediments, current flow indicators in imbricated fabric were measured at Bur-1 (27°34.01'N and 85°18.13'E), Bur-3 (27°34.34'N and 85°18.33'E), Bur-4 (27°34.359'N and 85°18.490'E), and Burs-1 (27°34.276'N and 85°18.067'E). The data set indicate that the vector mean of transportation direction of the sediments are towards N46°, N1° and N328°, respectively, at locations Bur-1, Bur-3 and Bur-4, while the mean vector flow is towards N129° at Burs-1 (Fig. 4).

Pyangaon site

The Pyangaon site lies between latitude 27°35'30.01''N to 27°35'54.59''E and longitude 85°19'39.74''N to 85°19'59.08''E. Seven lithological logs were extracted along a section from southwest to northeast. The sediment deposit at this site generally discloses upper coarse and lower fine sediment assemblages that are separated by a major erosional surface (MES) (Fig. 6). Thus, the lithofacies are categorized in the Pyangaon site as lower fine-grained facies and upper coarse-grained facies, however, in log Py-3 and Py-4 the coarse grained facies appeared at different time event below the MES.

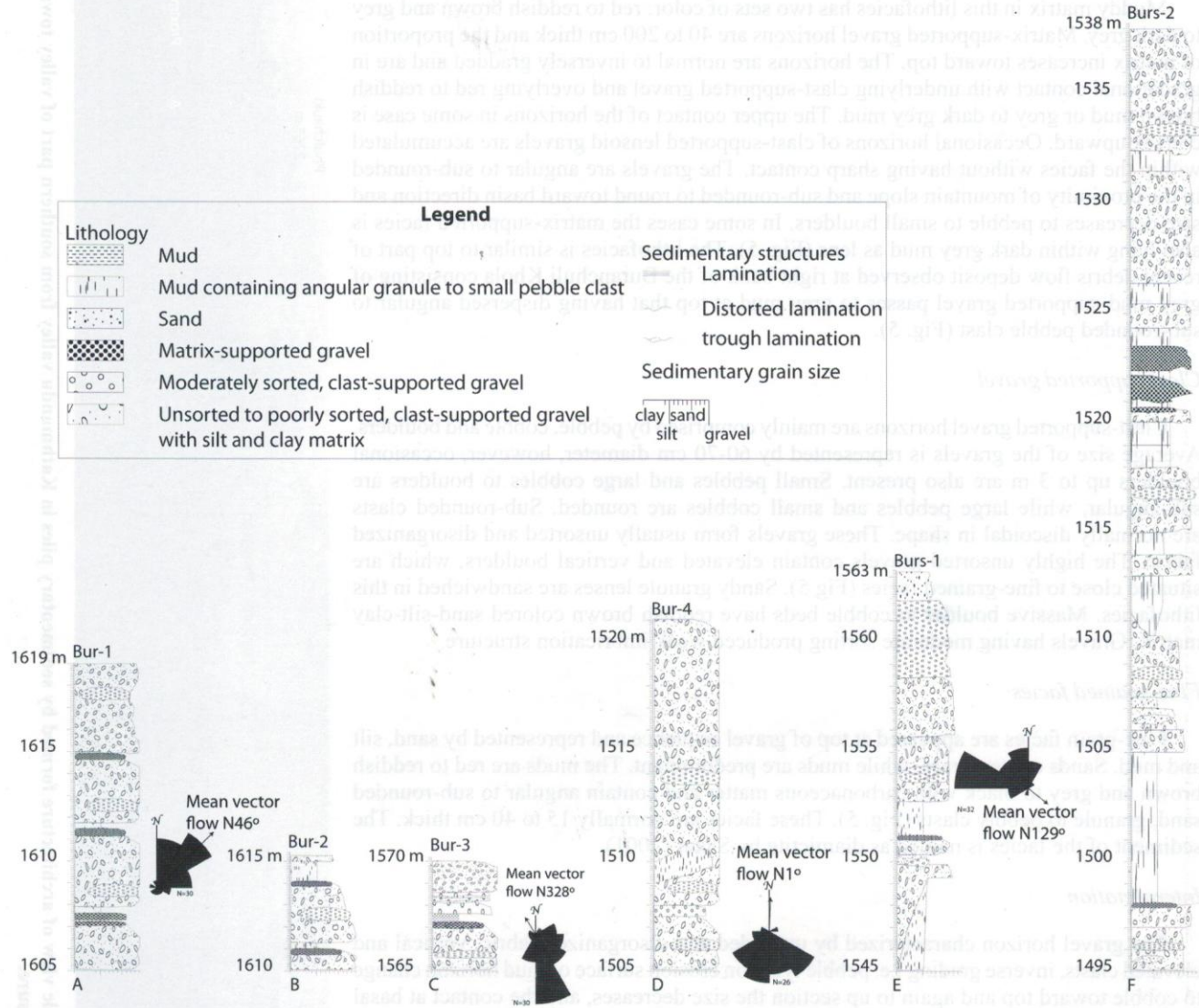


Fig. 4: Columnar section observed at Buranchuli site. (A) Bur-1 at latitude 27°34.276'N and longitude 85°18.067'E. (B) Bur-2 at latitude 27°33.97'N and longitude 85°17.95'E. (C) Bur-3 at latitude 27°34.34'N and longitude 85°18.33'E. (D) Bur-4 at latitude 27°34.359'N and longitude 85°18.490'E. (E) Burs-1 at latitude 27°34.276'N and longitude 85°18.067'E. (F) Burs-2 at latitude 27°34.346'N and longitude 85°17.991'E. Bar daigrams show pebble inclination direction, thus the flow is opposite to it.

Table 2: Geochronological data obtained from basin-fill sediments of Kathmandu valley compiled from various sources

Geochronology	Location	Dating material	Dating Method	Age		Lab code	Formation	Altitude	Source
				AMS	Conventional				
¹⁴ C	Santi Basti	Black silt	AMS	29,210		-	Kalimati	1,270	Fuji and Sakai 2002
	Rabibhawan ^a	organic carbon	AMS	44280*		-	Kalimati	1,273	Hayashi et al. 2009
	Rabibhawan ^a	organic carbon	AMS	40440*		-	Kalimati	1,275	Hayashi et al. 2009
	Rabibhawan ^a	organic carbon	AMS	33880*		-	Kalimati	1,277	Hayashi et al. 2009
	Rabibhawan ^a	organic carbon	AMS	35640*		-	Kalimati	1,278	Hayashi et al. 2009
	Rabibhawan ^a	organic carbon	AMS	32080*		-	Kalimati	1,280	Hayashi et al. 2009
	Bir Hospital	Black silt	AMS	15,620	±40 years	-	Kalimati	1,280	Fuji and Sakai 2002
	Rabibhawan ^a	organic carbon	AMS	28220*		-	Kalimati	1,281	Hayashi et al. 2009
	Rabibhawan ^a	organic carbon	AMS	22240*		-	Kalimati	1,283	Hayashi et al. 2009
	Rabibhawan ^a	organic carbon	AMS	20220*		-	Kalimati	1,284	Hayashi et al. 2009
	Rabibhawan ^a	organic carbon	AMS	19040*		-	Kalimati	1,286	Hayashi et al. 2009
	Rabibhawan ^a	organic carbon	AMS	12900*		-	Kalimati	1,293	Hayashi et al. 2009
	Thimi	Wood	Conventional	38,265	±1,230 years	Ly-9342	Thimi	1,297	Gajurel 2006
	Sano Thimi	Wood fragment	AMS	34,820	±400 years	JNC3889	Thimi	1,300	Sakai et al. 2008
	Sano Thimi	Wood fragment	AMS	33,995	±370 years	JNC3890	Thimi	1,300	Sakai et al. 2008
	Sinamangal	Pine cone	AMS	14190*	±110 years	JNC4658	Patan	1,300	Sakai et al. 2008
	TIA north	Wood fragment	AMS	40,320	±740 years	JNC4659	Thimi	1,300	Sakai et al. 2008
	Kapan	Wood fragment	Conventional	42,880	±910 years	JNC4660	Gokarna	1,300	Sakai et al. 2008
	Thimi	Bark	Conventional	29,290	±1,390 years	Ly-11189	Thimi	1,304	Gajurel 2006
	Thimi	Charcoala	Conventional	45,140	±1,310 years	Lyon-509 (Oxa)	Thimi	1,306.50	Gajurel 1998
	Thimi	Wood	AMS	21,650	±250 years	Lyon-1957 (Poz)	Thimi	1,307	Gajurel 2006
	Sano Thimi	Wood fragment	AMS	29,545	±290 years	JNC3891	Thimi	1,310	Sakai et al. 2008
	Gothatar	Wood fragment	AMS	39,160	±320 years	JNC4356	Gokarna	1,310	Sakai et al. 2008
	Kapan	Wood fragment	AMS	44,855	±1090 years	JNC4664	Gokarna	1,310	Sakai et al. 2008
	Kalimati	Wood fragment	AMS	12845*	±40 years	PLD5941	Kalimati	1,310	Sakai et al. 2008
	Thimi	-	Conventional	41,700	±5,600/3,200 years	VRI-1980	Thimi	1,311	Paudyal and Ferguson 2004
	Adhikarigaon	Lignite	Conventional	>43,000	years	-	Kalimati	1,315	Gajurel 1998
	Thimi	-	Conventional	>37,900	years	VRI-1979	Thimi	1,318	Paudyal and Ferguson 2004
Koteswor	-	-	11,070	±290 years	Gak-6201	Patan	1,318	Mugnier et al. 2011	
Koteswor	-	-	13,140	±380 years	Gak-6200	Patan	1,319	Mugnier et al. 2011	
Thimi	Charcoala	AMS	36,270	±930 years	AA-50056	Thimi	1,319.50	Gajurel 2006	
Manmajju	Trapa seed	AMS	47,635	±1460 years	JNC4665	Gokarna	1,320	Sakai et al. 2008	
Balaju	Charcoala	AMS	47,300	±2,900 years	AA-50065	Gokarna	1,320	Gajurel 2006	
Airport	-	-	14,050	±250 years	VRI-390	Patan	1,320	Franz and Kral 1975	
Thimi	Charcoala	Conventional	43,180	±1,160 years	Lyon-508(Oxa)	Thimi	1,320.50	Gajurel 1998	
Banyatar	Charcoala	AMS	48,700	±3,700 years	AA-50058	Gokarna	1,321	Gajurel 2006	
Arubari	Lignite	-	48,700	±3,200 years	-	Gokarna	1,321	Gajurel 2006	
Banyatar	Lignite	AMS	40,000	±1,300 years	AA-50062	Gokarna	1,322	Gajurel 2006	
Thimi	Charcoal	AMS	33,860	±610 years	AA-50057	Thimi	1,326	Gajurel 2006	
Dharmasthali	Wood roots	AMS	44,600	±360 years	PLD5942	Gokarna	1,328	Sakai et al. 2008	
Sinamangal	Pinecone	AMS	24,100	±80 years	-	Thimi	1,328	Sakai et al. 2008	

Geochronology	Location	Dating material	Dating Method	Age	Lab code	Formation	Altitude	Source
	Dharmasthali	Reed roots	AMS	43,270	PLD5943	Gokarna	1,329	Sakai et al. 2008
	Sinamangal	Pinecone	AMS	24,480	-	Thimi	1,330	Sakai et al. 2008
	Dharmasthali	Wood roots	AMS	>51,600	PLD5944	Gokarna	1,335	Sakai et al. 2008
	Sinamangal	Pinecone	AMS	24,540	-	Thimi	1,335	Sakai et al. 2008
	Sangla Khola	Wood roots	AMS	46,775	PLD5936	Gokarna	1,338	Sakai et al. 2008
	Dharmasthali	Wood fragment	AMS	35,490	JNC3892	Gokarna	1,340	Sakai et al. 2008
	Banyatar	Charcoal	AMS	>49,900	AA-50059	Gokarna	1,341	Gajurel 2006
	Dharmasthali	Wood fragment	AMS	45,630	JNC4667	Gokarna	1,345	Sakai et al. 2008
	Sangla Khola	Wood fragment	AMS	27,220	PLD5937	Thimi	1,345	Sakai et al. 2008
	Baniyatar-Baluwa	Wood roots	AMS	48,065	PLD5945	Gokarna	1,345	Sakai et al. 2008
	Dhapasi	-	-	49,300	GrN-23318	Gokarna	1,345	Paudyal 2002
	Dhapasi	-	-	>36,100	VRI-1981	Gokarna	1,345	Paudyal 2002
	Bicharithok	Wood fragment	AMS	42,385	JNC4661	Gokarna	1,350	Sakai et al. 2008
	Kabhresthali	Wood fragment	AMS	45,600	PLD5935	Thoka	1,350	Sakai et al. 2008
	Sunakothi	Charcoal	AMS	47,900	AA-50064	Gokarna	1,351	Gajurel 2006
	Baniyatar-Baluwa	Peat	AMS	53,040	PLD5946	Gokarna	1,355	Sakai et al. 2008
	Bicharithok	Wood fragment	AMS	54,515	JNC4657	Gokarna	1,360	Sakai et al. 2008
	Dharmasthali	Wood fragment	AMS	43,205	JNC4663	Gokarna	1,360	Sakai et al. 2008
	Dharmasthali	Wood fragment	AMS	17,180*	JNC4666	Thoka	1,360	Sakai et al. 2008
	Dharmasthali	Wood roots	AMS	46,420	PLD5939	Thoka	1,360	Sakai et al. 2008
	Sangla Khola	Wood fragment	AMS	14,250*	PLD5938	Thoka	1,363	Sakai et al. 2008
	Dharmasthali	Wood	AMS	49,595	PLD5940	Thoka	1,365	Sakai et al. 2008
	Sankhu	Lignite	Conventional	>44,000	-	Gokarna	1,370	Gajurel 1998
	Besigaon	plant nut	AMS	53,170	-	Gokarna	1375	Bhandari et al 2011
	Mulpani	Wood fragment	AMS	34,480	JNC3893	Gokarna	1,380	Sakai et al. 2008
	Bicharithok	Roots	AMS	19,380*	JNC4662	Thoka	1,400	Sakai et al. 2008
	Chunigaon	organic mud	Conventional	37,100	Beta-140259	-	1,420	Saijo and Kimura 2007
	Chunigaon	organic mud	Conventional	>40,300	Beta-140260	-	1,423	Saijo and Kimura 2007
	Bhusinkhel	organic mud	Conventional	29,190	Beta-135432	-	1,431	Saijo and Kimura 2007
	Bhusinkhel	organic mud	Conventional	>36,940	Beta-135433	-	1,432	Saijo and Kimura 2007
	Bhusinkhel	organic mud	Conventional	37,130	Beta-135434	-	1,433	Saijo and Kimura 2007
	Sundarjal	organic mud	Conventional	33,220	Beta-135435	-	1,435	Saijo and Kimura 2007
	Matikhel	organic mud	Conventional	32,160	Beta-140257	-	1,460	Saijo and Kimura 2007
	Thimi	-	-	45,300	KSU-1120	Thimi	1306~	Igarashi et al. 1988
	Thimi	-	-	37,200	KI-808	Thimi	1322.3~	Vishnu-Mittre and Sharma 1984
	Thimi	-	-	15,070	KI-807	Thimi	1326~	Vishnu-Mittre and Sharma 1984
	Thimi	carbonaceous clay	-	25,740	KI-806	Thimi	1327~	Vishnu-Mittre and Sharma 1984
	Kharipati	wood	-	29,200	VRI-608	Thimi	1340~	Kral and Havinga 1979
	Sankhu	-	-	>40,000	PRL-196	Gokarna	1370~	Vishnu-Mittre and Sharma 1984
	Sankhu	-	-	>40,000	PRL-193	Gokarna	1371~	Vishnu-Mittre and Sharma 1984
	Sankhu	-	-	>40,000	PRL-194	Gokarna	1371~	Vishnu-Mittre and Sharma 1984
	Sankhu	-	-	>40,000	PRL-195	Gokarna	1371~	Vishnu-Mittre and Sharma 1984
	Sankhu	-	-	17,400	PRL-192	-	1374~	Vishnu-Mittre and Sharma 1984

¹⁴C

Geochronology	Location	Dating material	Dating Method	Age	Lab code	Formation	Altitude	Source
¹⁴ C	Sankhu	plant remain	-	30,490	-	Gokarna	1390~	Dill et al. 2003
	Teku	-	Conventional	±1,070/1,320 years	Gak-6194	Patan	-	Yonechi 1976
	Teku	-	Conventional	±820 years	Gak-6193	Patan	-	Yonechi 1976
	Teku	-	Conventional	±1,050 years	Gak-6195	Patan	-	Yonechi 1976
	Koteswor	-	Conventional	±1,480 years	Gak-6201	Patan	-	Yonechi 1976
	Koteswor	-	Conventional	±290 years	Gak-6200	Patan	-	Yonechi 1976
	Suyaltal	-	Conventional	±380 years	Gak-6196	-	-	Yonechi 1976
	Suyaltal	-	-	>26,570 years	Gak-6197	-	-	Yonechi 1976
	Patan	-	-	>26,650 years	Gak-6198	-	-	Yonechi 1976
	Khajahl	-	-	±2,500/1,940 years	Gak-2875	-	-	Yonechi 1976
	Nakhu Khola	-	-	±6,100/3,400 years	-	Thimi	-	Yonechi 1973
	Chobhar	-	-	±960/1,090 years	-	Kalimati	-	Dill et al. 2001
	Patan	-	-	±1,310 years	Gak-6199	-	-	Dill et al. 2003
	Pashupati	-	-	>23,390 years	TH-729	Patan	-	Yonechi 1976
	Chainakhel	plant remain	Conventional	±390/360 years	-	Kalimati	-	Yoshida and Igarashi 1984
	Thimi	Plant debris	-	±1,470/1800 years	-	Thimi	-	Dill et al. 2003
	Gokarna	-	-	±1,665 years	-	-	-	Dill et al. 2001
	Gokarna	-	-	±1,960 years	Gak-5963	-	-	Yoshida and Igarashi 1984
	Gokarna	-	-	±2,600/2,000 years	Gak-6020	-	-	Yoshida and Igarashi 1984
	Gokarna	-	-	±2,660/2,040 years	Gak-5962	-	-	Yoshida and Igarashi 1984
Sankhu	-	-	±3,220/2,285 years	TF-189	Gokarna	-	Bösch 1974	
Thatipipal	-	-	>780 ka	-	Dharmasthali	1,400	Gautam et al. 2001	
Lukundol	-	-	2.9 Ma - <730 ka	-	Lukundol & Itaiti	-	Yoshida and Gautam 1988	

* calibrated age

~ altitude relocated according to map and text of source paper

a Core sample

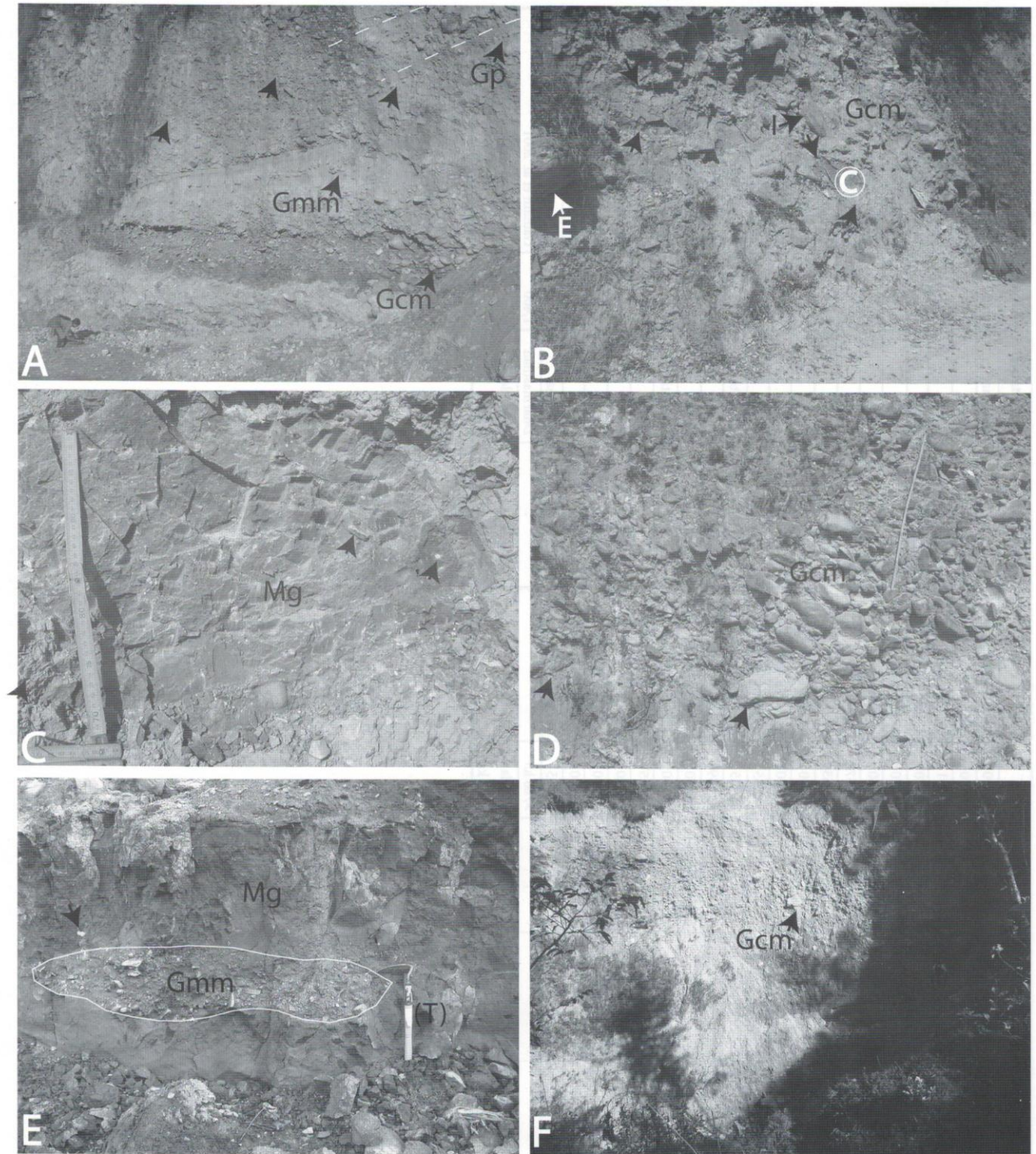
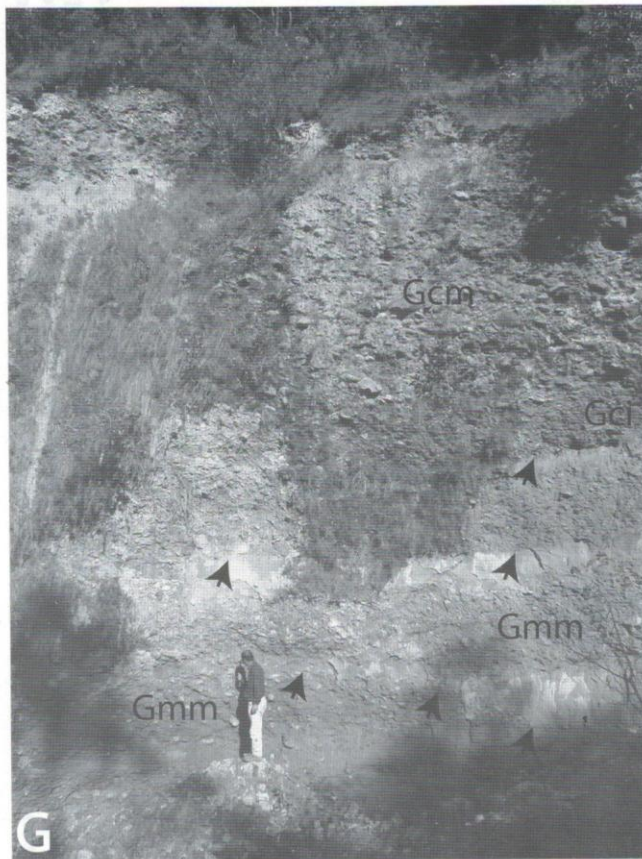


Fig. 5: Field photographs from Buranchuli area with lithofacies interpretation according to Miall (1996). (A) cross-bedded gravel deposit (Gp), matrix-supported massive gravel (Gmm), and Clast-supported massive gravel (Gcm). (B) Unsorted, clast-supported massive gravel (Gcm) having elevated (E) and highly inclined (I) boulders. Angular rock-fragments bearing mud (Mg) layer is marked by black arrow and details of 'c' mark is shown in photo (C). (C) Reddish brown mud (Mg) having angular to sub-rounded gravels marked by black arrow. (D) Moderately sorted, clast-supported massive gravel (Gcm) with imbrication fabric. Black arrows delimit mud and gravel zones. (E) Angular rock-fragments bearing dark grey mud (Mg) enclosed matrix-supported angular massive gravel (Gmm). Scale of tool (T) is 33 cm in length. (F) Unsorted, angular to sub-rounded, clast-supported massive gravel (Gmm).

contd....

.... contd



(G) Debris flow deposit in the Itaiti Formation; lithofacies inversely graded, clast-supported gravel (Gci), Gcm and Gmm. Note the convex upward contact Gmm at the base of photograph marked by three arrows and the planar to undulating contact between gravel and mud marked by a single and two arrows. (H) Recent debris flow deposit of Buranchuli Khola; lithofacies matrix-supported massive gravel (Gmm) overlain by angular rock-fragments bearing mud (Mg).

Lower fine-grained facies

The lower fine-grained facies are represented by 2 to 30 cm thick, very fine- to medium-grained, grey to reddish yellow sand, 2 to 50 cm thick, light yellow to dark grey silt and 2 to 200 cm thick, light to dark grey silty clay. Sand and silt are massive to parallel, cross- and current-ripple laminated and silty clays are massive to parallel laminated. Laminae are comprised by very fine sand, silt, clay and organic matter and are disrupted and distorted due to organic activity. Very fine-grained sand and silt are also rhythmically alternating. Sporadic plant debris is dispersed in fine sediments. Up to 6 cm deep burrows are frequently observed particularly in silty sediments and are slight to vertical in inclination. 5 to 20 cm thick gravel layer is consisting of angular to rounded pebble-cobble size clasts comprised by sandstone.

Interpretation

These facies are interpreted as a deposit in delta plain, delta front and pro-delta environments (Fig. 6). In the delta plain deposit, the facies is characterized by gravel, very fine-grained sand and silty clay. Pebbly clasts are

dispersed in sand, silt and clay matrix. Gravel level contains dominant pebble of sand stone and also reveals very angular intraformational mud clasts and plant debris. At upstream section it is associated with slumped and micro-faulting up to 14 cm in displacement at location Py-1 (27°35'40.33"N and 85°19'25.43"E), where parallel to buckled laminated, medium-grained sand layer contains rounded granule and pebble of high sphericity. Sand lenses in silt and silty clay are frequent at upper part of the deposit. The top layer is often mottled and bioturbated and consists of carbonized wood fragment and rootlets.

In delta front deposits, massive to parallel and ripple cross-laminated, very fine- to fine-grained sand and silt disclose roots, bioturbation and burrow structures. The laminae are often distorted and interrupted and the sediments are sometime mottled. Large to small carbonized wood fragments are also accumulated in the sediments (Fig. 7).

Pro-delta deposits are characterized by alternation of massive, parallel to ripple cross-laminated, very fine sand, silt and silty clay. Sands are generally very thin and their proportion is much lesser than silt and silty clay. Small

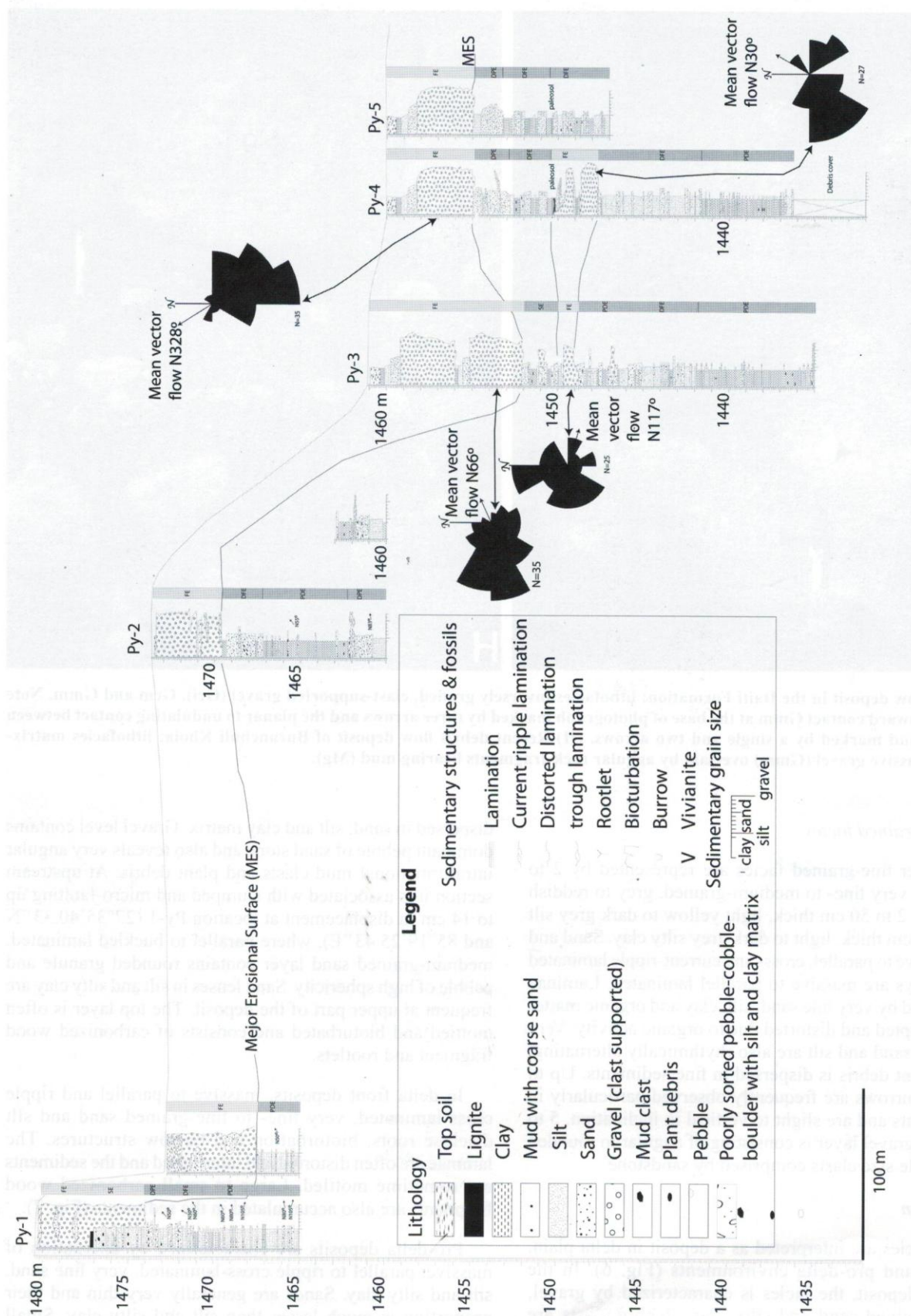


Fig. 6: Columnar cross-section along Py-1 (27°35'40.33"N and 85°19'25.43"E), Py-2 (27°35'41.17"N and 85°19'40.79"E), Py-3 (27°35'48.48"N and 85°19'44.70"E), Py-4 (27°35'52.30"N and 85°19'48.94"E) and Py-5 in Pyangon area. The abbreviation for environmental interpretation is decoded as: FE- Fluvial environment, SE- Swamp environment, DPE- Delta plain environment, DFE- Delta front environment, DFE- Pro-delta environment. Rose diagrams for current flow direction represent the immediate right lithofacies of columnar section at same level of position. Bar daigrams show pebble inclination direction, thus the flow is opposite to it. Section height is given in altitude from above mean sea level in m.

fragments of carbonized wood are sparsely dispersed in the sediments and in some cases organic matter also develops laminae in silty clayey sediments. Silty sediments are often bioturbated. Blue colored vivianite is occasionally found in silty clayey sediments.

A sequence is characterized by a 3 to 5 cm thick, parallel laminated, massive to graded, fine to medium-grained, reddish light yellow sand having undulating erosive basal surface is overlain by a 3 to 5 cm thick current ripple laminated very fine sand, which is covered by 0.5 to 2 cm thick parallel laminated very fine sand and silt with 0.5 to 1 cm thick, massive grey muddy silt and silty clay at top. The basal sandy horizon sometimes also contains scattered pebbles (6 x 3 x 2 cm). Such sequence is interpreted as a complete sequence of turbidite (Fig. 7). These sequences are found in the deposit of lacustrine environment.

5 to 7 cm thick, matrix supported, gravel horizon having planer to undulating basal contact with delta front deposit consisting of interbedded, very fine-grained sand, silt and clay and irregular contact with overlying silty clay and sandy lenses is interpreted as sub-aqueous debris flow deposit (Fig. 7). The deposit is consisting of sub-angular to rounded extraformational pebbles and deformed intraformational angular mud clasts. Matrix is comprised by sand, silt and clay.

The sediments composed of laminated, fine-grained sands, dark grey muddy mottled silt having carbonized wood fragments, rootlets, and bioturbation structures and thin layer of lignite at top are interpreted as a deposit of swampy area in the delta plain environment. Directions of sediment transport measured in cross-laminae of fines grained facies indicate from N30° to N105° (Fig. 6).

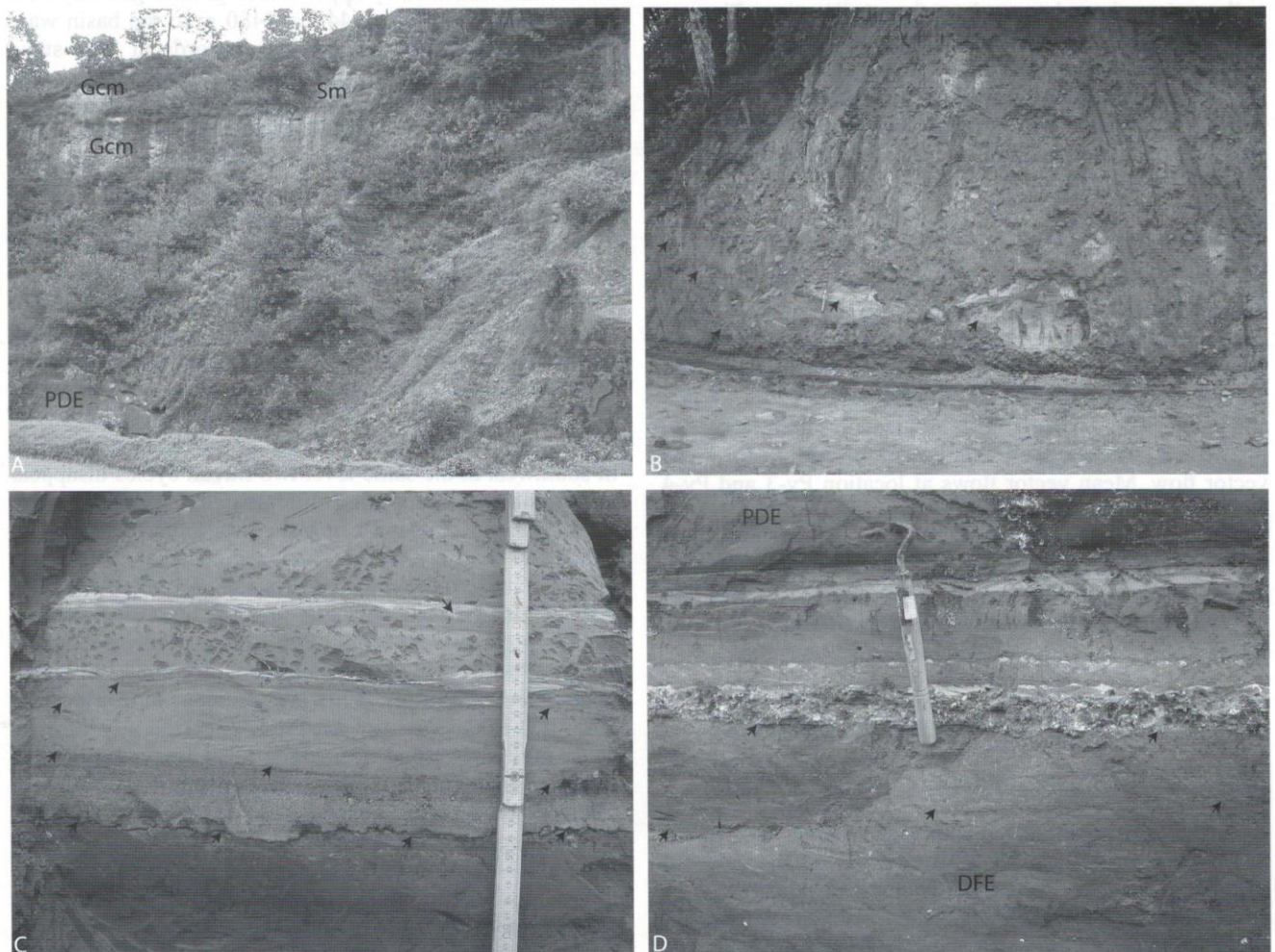


Fig. 7: Field photograph from Pyangaon area. (A) Example of exposure in Py-3 site, clast-supported massive gravel (Gcm), massive, fine- to coarse-grained sand (Sm) and lithofacies related to pro-delta environment (PDE). (B) Intraformational angular clasts shown by black arrow and three arrows at left indicate paleo-river/bank of gravelly river system. (C) Example of turbidite sequence; base of sequence is marked by four arrows, top of faint laminated sand is marked by three arrows; top of ripple-cross laminated horizon is marked by two arrows; top decanted massive silty clay is marked by single arrow; downward indicating arrow shows deformed laminae in sand. (D) Deposit of delta front environment (DFE) and pro-delta environment (PDE); three arrows at best mark the inclined surface of silt and fine sand lithofacies, two arrows mark sub-planar to undulating contact at base of debris flow produced due to high shear friction.

Upper coarse-grained facies

The coarse grained facies assemblages are more than 4 m thick and normally have distinct MES at its basal part that separates from lower fine-grained facies, however it appears below MES as different time events in Py-3 and Py-4 (Fig. 6). It is comprised by sub-rounded to rounded and generally discoidal shaped pebble, cobble and boulders (20 x 10 x 8 cm maximum) embedded in sand, silt and clay matrix. The gravels are characterized by normally massive clast-supported fabric with imbrication structure. Granule to pebble supported and pebble to cobble supported lens develop both normal and reverse grading. The clasts are composed of mostly sandstone derived from southern metasedimentary terrain. In some places, it contains up to a meter large angular fragments of lower fine-grained facies, which could be derived from bank collapses (Fig. 7). Erosional bank scar at Py-3 above MES slopes around 62° due N140°, which means valley was oriented toward northeast direction. Fine- to coarse-grained, massive to cross-laminated, light grey sand and silty mud lens up to 110 cm thick are found in the gravel layer. The upper coarse-grained facies assemblages end at top with fine- to coarse-grained, massive sand and grey clayey silt with rootlet and plant debris. Basal depositional contact dips 10° due N120°.

Interpretation

The gravelly lithofacies is interpreted as river channel deposit fed by basin ward propagating high energy water current in alluvial fan that developed at the southern headwater area of the basin indicating a humid climatic regime with enough precipitation (Carling 1996; Shukla and Bora 2005). Measurement of paleocurrent directions on imbricated structure show highly variable values for mean vector flow. Mean vector flows at location Py-3 and Py-4 show the transportation direction towards N30° to N117° for the deposit below MES and N66° and N328° for gravel beds situated above MES (Fig. 6). These deposits could be the product of gravelly meandering river similar to present day Godavari Khola located to eastern part of Pyangaon area, which flow from south-southeast to north at basin center.

DISCUSSION AND CONCLUSION

Deposition environmental fluctuation

Kathmandu basin has accommodated around 600 m thick sediments (Moribayashi and Maruo 1980). At the southern part of the basin the pattern of sedimentary piles reveal an area of alluvial fan system with gently inclined depositional surfaces (Fig. 3). Grain size analysis performed in micro-granulometric laser Malvern model-215 at the University of Chambéry, France for less than 1 mm matrix sampled at location Da 4 (27°35'3.55"N; 85°17'4.5"E; 1260 m) from the deposit show the proportion of sand:silt:clay as 32:47:21% (Table 3). Gravels at the area is interpreted as debris flow deposit (Gajurel 1998).

In Buranchuli area, the basin-fill deposit from 1500 to 1620 m amsl is comprised by monotonous several cycles of thick, coarse-grained sediments (gravels) that terminate toward the top by fine-grained muddy sediments. In fact, to the proximal fan area sediments were accumulated mostly in debris flow and normal river current flow conditions (e.g. Bull 1972). Toward the basin center these sediments are associated with lacustrine sediments in inter-fingering relationship. In contrast, the sediments in the Pyangaon area are clearly distinct into upper coarse-grained and lower fine-grained facies associations. Between 1477 and 1435 m amsl in the area, lower fine-grained facies association represent delta plain, delta front and prodelta sub-environment, while first delta plain sub-environment is found between 1477 and 1473 m. The record of first delta front sediment starts at 1473 m that mimics the high stand paleo-lake level in southern part of Kathmandu basin. In fact, the fine-grained facies is eroded and truncated by upper coarse-grained gravelly river facies association from 1448 to 1480 m to the basin ward direction. Therefore, sedimentary records of high stand lake level in the Pyangaon area are not preserved. However, decreasing level of MES clearly depicts the increasing surface area of sub-aerial environment within the Kathmandu basin. Lithological logs extracted from the extreme northward direction of basin in the study area (Py-4 and 5) reveal distinct two cycles of gravelly river deposit that start from 1448 m is characterized by fining upward sequence (Fig. 6). The upper cycle is ended around 1449.50 m by paleosol consisting of very fine-grained, reddish yellow sand and silt with rootlets. The paleosol is covered by very fine-grained, reddish yellow sand and silt having parallel- and ripple-cross laminae and burrow structures, which is interpreted as delta front deposit. Toward top, delta plain sediments of about 2 m thickness are preserved. To a distance of about 30 m southwest at the same level two fluvial cycles disappear and replaced by a deposit of bioturbated, very fine-grained sand, silt and clay with burrow structures, where plant debris and roots are found. These sediments are massive to parallel- and cross-laminated. Black silty clay, black clay, light to dark grey silt, very fine-grained, light grey sand are alternating. Laminae are often distorted. These sediments are covered by the same paleosol observed at 1449.5 m. Toward top, delta front facies is continuous in this location also. It means lake was lowered, consequently erosion occurred (gravel) and again lake level was raised (delta front deposit). Thus, the sub-aerial deposition environment changed sub-aqueous deposition system toward the higher level. It suggests that at least 5 m lake level was raised. At around 1,440 m, increase in smectite (50%) corroborates for the blockade in drainage system of the basin (Table 3). Then again lake was lowered and erosion occurred (gravelly river system). The mechanism for the lake level fluctuation could be regulated by the alluvial fan aggradation system, and degradation thanks to erosion at the outlet of the Bagmati River in south. For example, paleocurrent directions at the Buranchuli area indicate sediment transportation towards basin center, however, occasional thick pulses of sediments (Burs-1 at 1555 m) were brought from northwest to southeast

Table 3: Grain size, clay mineral and oxygen isotopic composition of modern and basin-fill sediments

Sample No.	Geographical location		Altitude m amsl	$\delta^{18}O$ of sediment < 2 μ m	Clay mineralogical percentage in sediments from XRD						Size analysis for <1 mm in diameter		
	Latitude	Longitude			Illite (I)	Chlorite (C)	Kaolinite	Smectites (S)	I-S	C-S	Clay < 3.9 μ m	Silts	Sands
Sp 2	27°44'17.01"	85°27'60.00"	1425	16.9	20	0	73	0	4	3	Saprolite		
Sp 1	27°44'17.01"	85°27'60.00"	1419	16.3	8	0	74	5	8	5	Saprolite		
Jao-3	27°35'39.96"	85°18'20.14"	1380	Na	25	0	23	35	13	4	23	64	13
Da 10	27°35'47.46"	85°17'31.31"	1315	12.2	33	0	18	34	15	0	Na	Na	Na
Da 14	27°36'9.84"	85°17'37.02"	1265	11.7	18	0	25	36	14	7	6	21	73
Da 4	27°35'03.7"	85°17'4.23"	1230	Na	Na	Na	Na	Na	Na	Na	21	47	32

Source: Gajurel 1998

direction at the marginal basin parts. Debris flow as well as landslide occurrences at the basin outlet could play major role for plugging of Bagmati at south. Furthermore, the same mechanism could regulate for the establishment of various depositional delta plain and delta front terraces to the north at different time scale since the southern fan system is continuous in its record (Sakai et al. 2000; Gajurel 2006). Debris flows like Burs-1 at 1555 m elevation could be a major cause for the lacustrine sedimentation at around 1471 m in Pyangaon and around 1400 m in the Tiniple area (27°46'35'89" and 85°16'41.07"), where the altitude of col (about 1465 m) is found the lowest point in the water divide line of the Kathmandu basin (Saijo and Kimura 2007). The basin would be drained through the col to the Trishuli River system at the time of deposition (Fig. 1). Figure 8 summarizes the deposition environmental fluctuations, particularly, at northern part of the basin focusing on the fan sediments with altitude at the south.

Age paradox

Depositional ages of the sediments of Kathmandu basin-fill deposits (Table 2) have been established using ^{14}C -radiometric, paleomagnetic and paleontological methods. Long- and short-term lake level fluctuations in the Kathmandu basin have consequences as: first sediment mixing of two contrast ages that is revealed by reverse age pattern in normal order of superposition and second a large depositional time gap without having conspicuous erosional surfaces in normal order of superposition. There is plenty of ^{14}C age records of highly remobilized i.e. reworked sediments from previous deposits, particularly in the central part of the basin. Thus, such reworked sediments extremely confused ^{14}C -radiometric depositional age of sediments if a limited number of age data on hand. Furthermore, the mixing is occurred between the sediments of a short range, for example, stacking of sediments of 11, 830 – 13,390 years BP in reverse order of superposition in 1.25 m thick, carbonaceous clay in airport section or sediments of 17,270 – 13,710 years accumulated in 2 m thick carbonaceous clay at Nariwalphat (27°41'25.98" and 85°16'33.61") area (Vishnu-Mittre and Sharma 1984), and between the sediments of long age range, for example, at Thimi section 21 ka sediment appeared at middle part of a 25 m thick section, while to the upper part at the same section the sediments of greater than 45 ka reworked is mixing (Gajurel 1996; Paudel 2002; Igarashi et al. 1988). It means that the basin was intermittently subjected to active sedimentation as well as erosional processes during the course of basin filling. A large depositional gap between >40,000 and <17,400 years observed in sediments from Sankhu area further corroborates active sedimentation-erosion activity within the basin (Vishnu-Mittre and Sharma 1984; Gajurel 1998). Figure 9 summarizes sedimentation- erosion process within the Kathmandu basin.

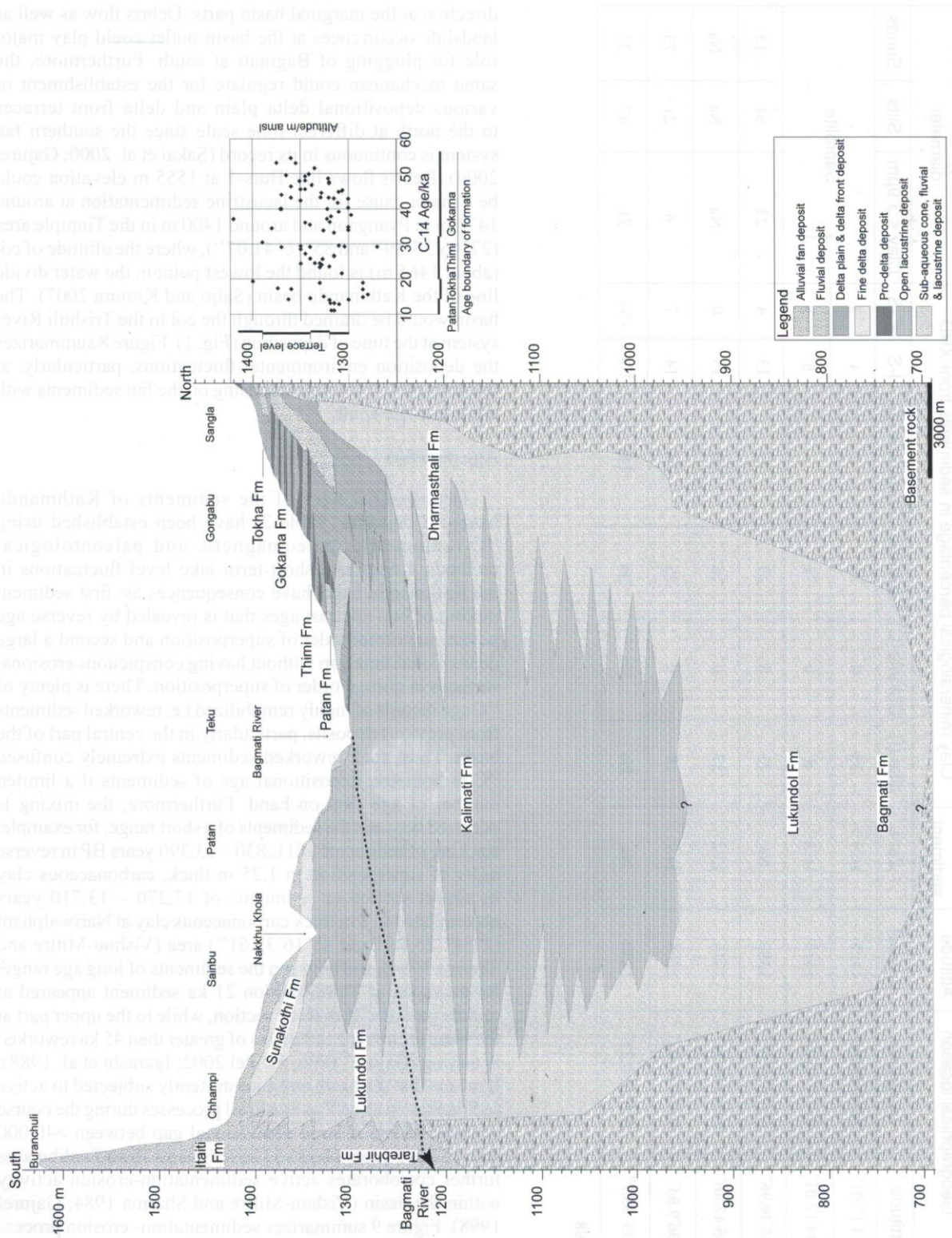


Fig. 8: Geological cross-section taken through the basin-fill sediments from Buranchuli-Chhampi-Patan-Teku-Gongabu to Sangla showing sediments of various depositional environments within the Kathmandu basin with ¹⁴C-age of upper part of sediments to rightside of the section.

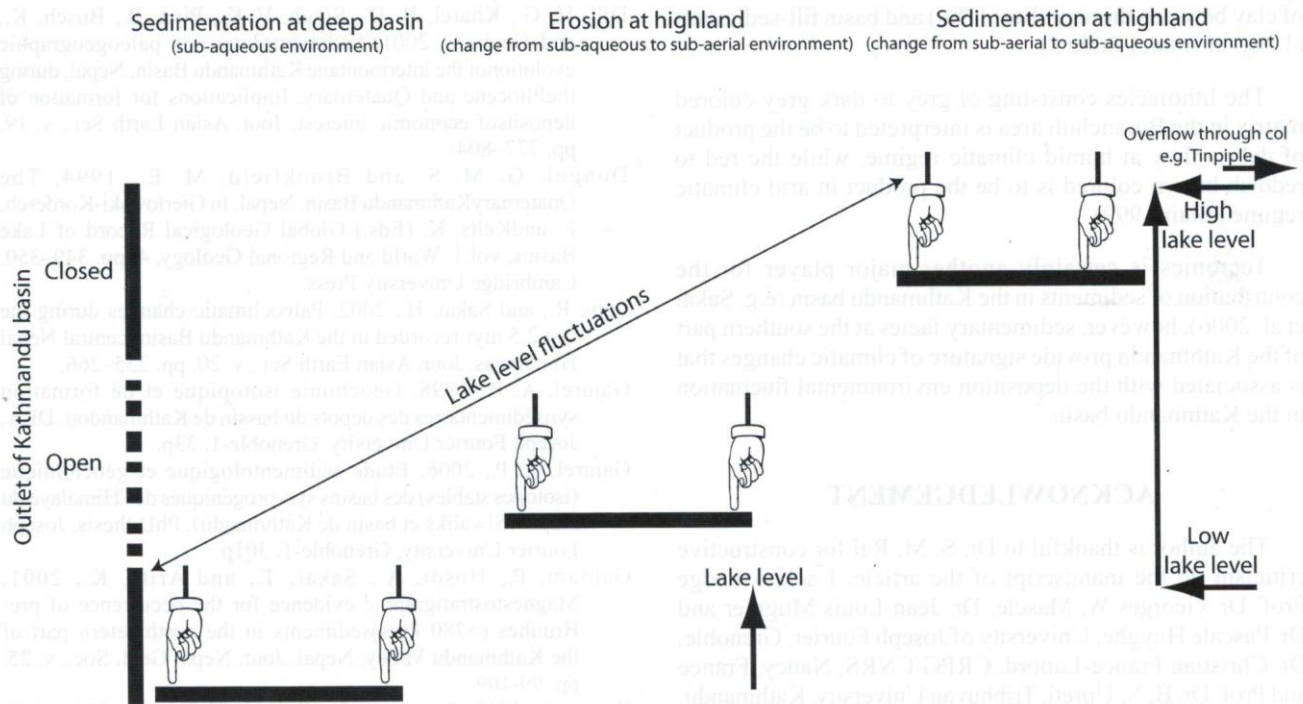


Fig. 9: Cartoon showing sedimentation-erosion location of Paleo-Kathmandu Lake during deposition environmental fluctuation.

Climate and Sedimentation

Pyangaon site is bordered by high mountainous (1766 to 2765 m) area, while the Buranchuli site covers larger watershed area of lower altitude. Sediment transportation in the Buranchuli site was predominated in the form of bed load as debris flow as well as normal river water current, while the sedimentation processes in the Pyangaon site was performed in the form of suspension load and decantation processes. Furthermore, Pyangaon site is located at the border of the lake near a sediment source with high relief area, however, record of debris flow events is rare. Lower fine-grained lithofacies association representing silty clay sediment of pro-deltaic sub-environment indicates a calm decantation process in sub-aqueous environment, while sandy sediments indicate activity of strong current i.e. monsoon rain. This cycle is interrupted by episodic pulses of sediment flux, for example, at level 1463, 1464, 1465, and 1466 m amsl in Py-2 location. Such sequences are the pulses of turbidity current flow at the marginal area of the basin. These deposits, in fact, represent a pulse of high-energy transportation process from considerable distance within a calm lacustrine environment since the pebbles are rounded in form, which mimic occurrence of intermittent heavy precipitation within the boundary of southern watershed of the Kathmandu basin.

The sediments in Thimi area represent deltaic and lacustrine environment with minor fluvial systems. Age data from Vishnu-Mittre and Sharma (1984) indicate that 3.7 m thick carbonaceous clay was accumulated between

15,070 and 37,200 years BP, which calculates the rate of sedimentation around 6 mm/yr, which is higher than in open lacustrine environment at Sundarighat (0.1 mm/yr) and Rabibhawan (0.18 to 1.2 mm/yr) (Fujii and Sakai 2001; Hayashi et al. 2009; Kuwahara et al. 2010). Considering the maximum sedimentation rate at Piyangaon site, 1 m thick sedimentation excluding compaction, suggests the lake level was stand for 165 years at locations Py-4 and Py-5 (Fig. 6). It means deposition environmental fluctuation had occurred for centennial scale.

During the wet climatic regime an intense chemical weathering and erosion of basement rock at the surroundings of the Kathmandu basin promote transformation of illite to kaolinite (Kuwahara et al. 2010). Clay mineral composition in saprolite sample developed on gneiss to the north of Sankhu (27°44'17.01"N and 85°28'0.04"E) illustrates more than 70% kaolinite and less than 5% smectite at the present day' monsoonal regime i.e. 1500 mm average annual precipitation (Table 3). In contrast, around 20 m thick grey mud that was deposited at the altitude of 1,315 m show increase in proportion of smectite and illite-smectite (50%) ratio in clay mineralogy at the southern part of the basin, which indicates a water logged condition probably caused by outlet plugging of the Bagmati River (Table 3). It means the climatic regime was represented by a dry climate interval with a poor drainage system in the area (Gajurel 1998; Kuwahara et al. 2010). Likewise, around 20 m thick grey mud deposited at around the altitude of 1,315 m show increase in proportion of smectite and illite-smectite (50%) ratio in clay mineralogy. The change is also indicated in $\delta^{18}\text{O}$

of clay between the saprolite (17%) and basin fill-sediments (12%) at south (Table 3).

The lithofacies consisting of grey to dark grey colored matrix in the Buranchuli area is interpreted to be the product of debris flow at humid climatic regime, while the red to reddish brown colored is to be the product in arid climatic regime (Blair 1999).

Tectonics is certainly another major player for the contribution of sediments in the Kathmandu basin (e.g. Sakai et al. 2006), however, sedimentary facies at the southern part of the Kathmandu provide signature of climatic changes that is associated with the deposition environmental fluctuation in the Kathmandu basin.

ACKNOWLEDGEMENT

The author is thankful to Dr. S. M. Rai for constructive criticism on the manuscript of the article. I acknowledge Prof. Dr. Georges W. Mascle, Dr. Jean-Louis Mugnier and Dr. Pascale Huyghe, University of Joseph Fourier, Grenoble, Dr. Christian France-Lanord, CRPG/CNRS, Nancy, France and Prof. Dr. B. N. Upreti, Tribhuvan University, Kathmandu, Nepal for their continuous support and fruitful discussion on the subject. The author is indebted to Dr. T. Sakai, Shimane University, Japan and Dr. H. Sakai, Kyoto University, Japan for valuable discussion and encouragement. The author is thankful for anonymous reviewers.

REFERENCES

- Bhandari, S., Paudyal, K. N., and Momohara, A., 2011, Late Quaternary plant macrofossil assemblages from the Besigaon section of the Gokarna Formation, Kathmandu Valley, central Nepal. *Jour. Nepal Geol. Soc.*, v. 42, pp. 1-12.
- Bajracharya, S. R., 1996, Morphostatistical analysis of the third order drainage basins of the Kathmandu valley, central Nepal. *Bull. Dept. Geology, Tribhuvan Univ., Kathmandu, Nepal*, v. 5, pp. 37-46.
- Blair, T. C., 1999, Sedimentology of debris flow dominated Warm spring Canyon alluvial fan, Death Valley, California. *Sedimentology*, v. 46, pp. 941-965.
- Bösch, H., 1974, Untersuchungen zur morphogenese im Kathmandu Valley. *Geographica Helvetica*, v. 29, pp. 15-26.
- Bull, W.B., 1972, Recognition of alluvial-fan deposits in the stratigraphic records. Pp. 63-83 in Rigby, J.K., and Hamblin, W.K., eds, Recognition of ancient sedimentary environments. Tulsa, Okla., Econ. Paleontologists and Mineralogists, Spec. Pub. No. 16, 340 p.
- Carling, P.A., 1996, Morphology, sedimentology and paleohydraulic significance of large gravel dunes, Altai mountains, Siberia. *Sedimentology*, v. 43, pp. 647-664.
- Dhondial, E. P., 1966, Investigation of lignite deposits in Kathmandu Valley, Nepal. Geological Society of India, report, 34 p.
- Dill, H. G., Khadka, D. R., Khanal, R., Dohrmann, R., Melcher, F., and Busch, K., 2003, Infilling of the younger Kathmandu-Banepa intermontane lake basin during the Late Quaternary (Lesser Himalaya, Nepal): a sedimentological study. *Jour. Quat. Sci.*, v. 18, pp. 41-60.
- Dill, H. G., Kharel, B. D., Singh, V. K., Piya, B., Busch, K., and Geyh, C., 2001, Sedimentology and paleogeographic evolution of the intermontane Kathmandu Basin, Nepal, during the Pliocene and Quaternary. Implications for formation of deposits of economic interest. *Jour. Asian Earth Sci.*, v. 19, pp. 777-804.
- Dongol, G. M. S. and Brookfield, M. E., 1994, The Quaternary Kathmandu Basin, Nepal. In Gierlowski-Kordesch, E. and Kelts, K. (Eds.) *Global Geological Record of Lake Basins*, vol.1. World and Regional Geology, 4, pp. 349-350, Cambridge University Press.
- Fujii, R., and Sakai, H., 2002, Paleoclimatic changes during the last 2.5 myr recorded in the Kathmandu Basin, central Nepal Himalayas. *Jour. Asian Earth Sci.*, v. 20, pp. 255-266.
- Gajurel, A. P., 1998, Géochimie isotopique et de formation sédimentaires des dépôts du bassin de Kathmandou. DEA, Joseph Fourier University, Grenoble-1, 33p.
- Gajurel, A. P., 2006, Etude sédimentologique et géochimique (isotopes stables) des bassins syn-orogéniques de l'Himalaya du Népal (Siwaliks et bassin de Kathmandu). PhD thesis, Joseph Fourier University, Grenoble-1, 301p.
- Gautam, P., Hosoi, A., Sakai, T., and Arita, K., 2001, Magnetostratigraphic evidence for the occurrence of pre-Brunhes (>780 kyrs) sediments in the northwestern part of the Kathmandu Valley, Nepal. *Jour. Nepal Geol. Soc.*, v. 25, pp. 99-109.
- Hagen, T., 1969, Report on the Geological Survey of Nepal. V. 1, Preliminary reconnaissance. *Denksch. Schweiz. Natur. Gesellschaft*, Zurich, v. 86, 185p.
- Holmes, A., 1978, Principles of Physical Geology. ELBS, Third edition, 730 p.
- Hayashi, T., Tanimura, Y., Kuwahara, Y., Ohno, M., Mampuku, M., Fujii, R., Sakai, H., Yamanaka, T., Maki, T., Uchida, M., Yahagi, W., and Sakai, H., 2009, Ecological variations in diatom assemblages in the Paleo-Kathmandu Lake linked with global and Indian monsoon climate changes for the last 600,000 yr. *Quaternary Research*, v. 72, pp. 377-387.
- Igarashi, I., Yoshida, M., and Tabata, H., 1988, History of vegetation and climate in the Kathmandu Valley. *Proceedings of the Indian National Science Academy* v. 54A, pp. 550-563.
- Kral, F., and Havinga, A.J., 1979, Pollenanalyse und Radiokarbon datierung an Proben der oberen Teile der Sedimentserie des Kathmandu-Sees und ihre vegetationsgeschichtliche Interpretation. *Sitzungsberichte. Abteilung I. O. österreichische Akademie der Wissenschaften. Mathematisch-Naturwissenschaftliche Klasse*, v. 188, pp. 45-61.
- Kuwahara, Y., Masudome, Y., Paudel, M. R., Fujii, R., Hayashi, T., Mampuku, M., and Sakai, H., 2010, Controlling weathering and erosion intensity on the southern slope of the Central Himalaya by the Indian summer monsoon during the last glacial. *Global and Planetary Change*, v. 71, pp. 73-84.
- Miall, A. D., 1996, The Geology of Fluvial Deposit, Sedimentary Facies, Basin Analysis and Petroleum Geology. Springer, Berlin, 582 p.
- Moribayashi, S., and Maruo, Y., 1980, Basement topography of the Kathmandu Valley, Nepal: an application of gravitational method to the survey of a tectonic basin in the Himalayas. *Jour. Japan Soc. Eng. Geol.*, v. 21, pp. 30-37.
- Mugnier, J.L., Huyghe, P., Gajurel, A.P., Upreti, B.N., and Jouanne, F., 2011, Seismites in the Kathmandu basin and seismic hazard in central Himalaya. *Tectonophysics*, v. 509, pp. 33-49.

- Natori, H., Takizawa, F., Motozima, K., and Nagata, S., 1980, Natural gas in the Kathmandu Valley. *Chishitsu News. Geology News from Geological Survey of Japan*, v. 312, pp. 24-35 (in Japanese).
- Nemec, W., and Steel, R. J., 1994, Alluvial and coastal conglomerates: their significant features and some comments on gravelly mass flow deposits. In *Sedimentology of gravels and conglomerates*, Koster, E. H., and Steel, R. J. (eds.), *Can. Soc. Petrol. Geol. Mem.*, v. 10, pp. 1-31.
- Paudyal, K.N., 2002, The Pleistocene environment of the Kathmandu Valley, Nepal Himalaya. Ph.D. Dissertation, University of Vienna, 157 p.
- Rai, S. M., 2001, Geology, geochemistry, and radiochronology of the Kathmandu and Gosainkund crystalline nappes, central Nepal Himalaya. *Jour. Nepal Geol. Soc.*, v. 25, pp. 135-155.
- Saijo, K., and Kimura, K., 2007, Expansion of an ancient lake in the Kathmandu basin of Nepal during the Late Pleistocene evidenced by lacustrine sediment underlying piedmont slope. *Himalayan Journal of Sciences*, v. 4(6), pp. 41-48.
- Sakai, H., Yahagi, W., Fujii, R., Hayashi, T., and Upreti, B.N., 2006, Pleistocene rapid uplift of the Himalyan frontal ranges recorded in the Kathmandu and Siwalik basins. *Palaeog. Palaeoclim Palaeoec.*, v. 241, pp. 16-27.
- Sakai, T., Gajurel, A. P., Tabata, H., Ooi, N., Takagawa, T., Kitagawa, H., and Upreti, B. N., 2008, Revised lithostratigraphy of fluvio-lacustrine sediments comprising northern Kathmandu basin in central Nepal. *Jour. Nepal Geol. Soc.*, v. 37, pp. 25-44.
- Sakai, H., 2001, Stratigraphic division and sedimentary facies of the Kathmandu Basin Group, central Nepal. *Jour. Nepal Geol. Soc.*, v. 25, pp. 19-32.
- Sakai, T., Gajurel, A. P., Tabata, H. and Upreti, B. N., 2001, Small amplitude lake level fluctuations recorded in aggrading deltaic deposits of the lower parts of the Upper Pleistocene Thimi and Gokarna Formations, Kathmandu Valley, Nepal. *Jour. Nepal Geol. Soc.*, v. 25, pp. 43-51.
- Sakai, T., Takagawa, T., Gajurel, A. P., Tabata, H., Ooi, N. and Upreti, B. N., 2006, Discovery of sediment indicating rapid lake-level fall in the late Pleistocene Gokarna Formation, Kathmandu Valley, Nepal: implication for lake terrace formation. *Daiyonki Kenkyu (Quaternary Research)*, v. 25(1), pp. 99-112.
- Sakai, T., Ooi, N., Takagawa, T., Gajurel, A. P., and Tabata, H., 2000, Reconstruction of depositional environment and paleoclimate change from the Quaternary basin fill succession of the Kathmandu Valley, Nepal. International seminar on Himalayan and Tibetan Uplift and Global Climate Change, program and abstract, Matsue, Shimane Prefecture, Japan, pp. 27-31.
- Shrestha, O. M., Koirala, A., Karmacharya, S. L., Pradhananga, U.B., Pradhan, R., and Karmacharya, R., 1998, Engineering and environmental geological map of the Kathmandu Valley (1:50,000) Dept. Mines and Geology, His Majesty's Government of Nepal.
- Shukla, U. K., and Bora, D. S., 2005, Sedimentation model for the quaternary intermontane Bhimtal-Naukuchiatal Lake deposit, Nainital, India. *Journal of Asian Earth Sciences*, v. 25, pp. 837-848.
- Stöcklin, J. and Bhattarai, K. D., 1981, Geological map of Kathmandu area and Central Mahabharat range (1: 250,000). Department of Mines and Geology, His Majesty's Government of Nepal, 64 p.
- Stuiver, M., Reimer, P. J., and Braziunas, T. S., 1998b, High precision radiocarbon age calibration for terrestrial and marine samples. *Radiocarbon*, v. 40(3), pp. 1127-1151.
- Stuiver, M., Reimer, P. J., Bard, E., Beck, J. W., Burr, G. S., Hughen, A., Kromer, B., McCormac, G., van der Plicht, J., and Spurk, M., 1998a, INTCAL 98 radiocarbon age calibration, 24,000-0 cal BP Radiocarbon, v. 40, pp. 1041-1083.
- Vishnu-Mittre, and Sharma, C., 1984, Vegetation and climate during the last glaciation in the Kathmandu Valley, Nepal. *Pollen et Spres*, v. 26, pp. 69-94.
- Yonechi, F., 1973, A preliminary report on the geomorphology of Kathmandu Valley, Nepal. *Sci. Dept. Tohoku. Univ. 7th Ser.*, v. 23, pp. 153-161.
- Yonechi, F., 1976, The basin landforms in Nepal. Preprint of Congress, Association of Japanese Geographers, v. 11, pp. 102-103 (in Japanese).
- Yoshida, M., and Gautam, P., 1988, Magnetostratigraphy of Plio-Pleistocene lacustrine deposits in the Kathmandu Valley, central Nepal. *Proc. Indian Nat. Sci. Acad.*, v. 54A, pp. 410-417.
- Yoshida, M., and Igarashi, Y., 1984, Neogene to Quaternary lacustrine sediments in the Kathmandu Valley, Nepal. *Jour. Nepal Geol. Soc.* v. 4, pp. 73-100.